BRINE CHEMISTRY AND PROPERTIES PREDICTION DURING SALAR EVAPORATION TO MAXIMIZE PRODUCT YIELD

By

Diana Miller and Anthony Gerbino

OLI Systems, Inc., USA

Presenter and Corresponding Author

Anthony Gerbino
aj.gerbino@olisystems.com

ABSTRACT

This paper outlines the use of the Mixed Solvent Electrolyte (MSE) model to predict the chemical composition and properties of salar brines during evaporation. The model has been validated using published peer reviewed experimental data of different salts containing Li-Na-K-Mg-Ca-Sr-B-SO_4-CO_3-Cl ions. The MSE model is able to predict the formation of thirty-four halides, forty-three sulfates, twenty-one carbonates, thirty-four borates, and three mixed-anion salts. This allows the simulation of the full evaporation process, from leaching to purification, of salars with different starting compositions.

Air evaporation of six salar brines from several geographic sources was simulated. We documented the progression of salt types as the brine volume decreases. Twenty-seven salts were predicted to precipitate and dissolve during the evaporation pathway. Several of these salts sequester Li and B, reducing the overall yield of these salable products. The simulation also predicted, the mass of each salt and the quantitative amount of Li and B lost to the solid phases.

We also simulated the effects of chemical addition (e.g. CaO, Na_2CO_3, MgO, oxalic acid, etc.) on the specific salt formation and identify which chemical additive optimizes Li and B product yield. We did not consider coprecipitation or surface adsorption effects.

The objective of this work is to aid the engineer in maximizing Li-product yield, depending upon the composition of the brine, and to increase the yield of sub-products like B and KCl via simulation of the evaporation process.

Keywords: Lithium, Salar, Brine, Evaporation, MSE, Electrolyte

INTRODUCTION

The global demand for lithium salts is expected to continue its growth trajectory as the production of electric cars is forecast to increase substantially over the next decade. As lithium gains importance, the need to develop or optimize processes for lithium extraction are of outmost importance[1].

Electrolyte thermodynamics is a useful tool for simulating lithium extraction from brine evaporation because of its ability to predict the most stable set of salts formed from a brine as temperature, pressure, and composition change. Salar brines are multicomponent electrolyte solutions with complex chemical speciation, strong non-ideality, and complex phase behavior (e.g. the formation of multiple hydrated salts or double salts and the presence of eutectic points). A comprehensive thermodynamic model, referred to as Mixed Solvent Electrolyte (MSE)-model, has been developed to calculate the phase equilibria and other thermodynamic properties for such brines[2–4]. The theory provides a thermodynamic foundation to explain the variation of precipitation in different salar brines, predict mineral equilibria in natural waters, and give insights in how the properties and composition of the brines will behave when mixed with natural water or brines of other compositions.

In this work, the MSE thermodynamic framework was used to study the phase equilibria, speciation and other thermodynamic properties of salar brines during the different steps of lithium evaporation and extraction. These brines contain alkali (Li^+, Na^+, K^+) and alkali earth (Mg^+, Ca^+, Sr^{+2}) metals, anions (Cl^-, SO_4^{-2}, Br^-, HCO_3^-) and weak acids (H_3BO_3). The steps in lithium recovery include leaching of the salar salts, evaporation, precipitation, chemical treatment, and finally lithium salt separation. Each step results in a different solution composition and concentration. This impacts speciation, ion activities, and solid-phase saturation.

This work presents the results of an effort to collect experimental data and develop a predictive thermodynamic model that covers salar brines chemistry. The MSE model will help scientists to study and understand the chemistry of these brines, help the experimentalists design more optimum experiments, and help engineers incorporate new ideas into their extraction/optimization design. This model will also help to improve the production yield of Li, B, K, and other salable products, minimizes operational costs and the environmental impact.

THERMODYNAMIC MODEL

The MSE-thermodynamic framework has been described in detail by Wang et al.[2,5], and therefore only a brief summary is given here. The electrolyte-containing liquid phase is represented by a combination of the Helgeson-Kirkham-Flowers (HKF) equation of state for standard-state properties and the MSE activity coefficient model for solution nonideality. Accordingly, the chemical potential of a species i in a liquid (electrolyte) phase is calculated as:

$$\mu_i^L = \mu_i^{L,0,x}(T,P) + RT \ln x_i \gamma_i^{x,*}(T,P,x) \quad (1)$$

where $\mu_i^{L,0,x}(T,P)$ is the standard-state chemical potential from the HKF theory[6,7], x_i is the mole fraction, and $x_i\gamma_i^{x,*}(T,P,x)$ is the activity coefficient from the MSE theory of Wang et al.[2], which accounts for long-range electrostatic, specific ionic, and short-range intermolecular interactions.

The properties of the gas phase are obtained from the Soave-Redlich-Kwong equation of state (SRK-EOS)[8] Equation (2). The chemical potential in the gas phase is then calculated as:

$$\mu_i^G = \mu_i^{G,0}(T) + RT \ln \frac{P y_i \varphi_i(T,P,y)}{P^0} \quad (2)$$

where $\mu_i^{G,0}(T)$ is the chemical potential of pure component i in the ideal gas state, y_i is the mole fraction, $\varphi_i(T,P,y)$ is the fugacity coefficient from the SRK-EOS, P is the total pressure, and $P^0 = 1\ atm.$

For the solid phase, the standard chemical potential, $\mu_i^{S,0}$, is obtained as a function of temperature from the solid-state standard state Gibbs free energies of formation, $\Delta G_f^{S,0}$, absolute entropies, $S^{S,0}$, and heat capacities as a function of temperature, $C_p^S(T)$.

A diagram that summarizes the MSE-model is shown in Figure 1.

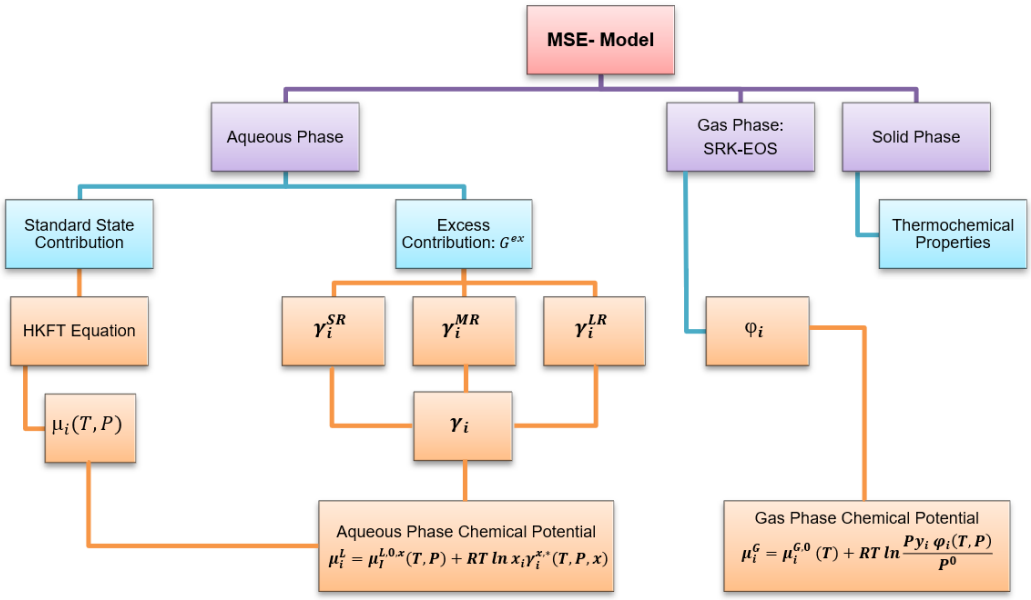

Figure 1. Structure of the MSE Framework

The solubility is a result of vapor-liquid (VLE) equilibria or solid-liquid equilibria (SLE), the latter being particularly relevant at atmospheric conditions. The VLE and SLE conditions are defined by the equality of the chemical potentials in the coexisting phases, i.e.,

$$\mu_i^L = \mu_i^G \ for\ VLE \tag{3}$$

$$\mu_i^S = \mu_i^L \ for\ SLE \tag{4}$$

The MSE calculations include: (1) the formation of ion pairs, complexes, etc.(chemical speciation), (2) the effect of electrostatic charge on each species in water (activity coefficients), (3) the availability of free water to form hydrates, (4) the intrinsic equilibrium constants (K-values) for each reactions as a function of temperature and pressure, and (5) the comprehensive list of single, double, triple salts, hydrated and anhydrous salts that may form. These five calculation elements are discussed through the paper.

MSE MODEL VALIDATION

The supporting database to the MSE framework was parameterized using 20,000+ experimental solubility measurements data from 100+ peer-reviewed papers for the subsystems of Li-Na-K-Mg-Ca-B-SO_4-CO_3-Cl-H_2O. These elements cover virtually 100% of a salar's brine mass. The model is validated for temperatures between -10 and 300°C, and salt concentrations up to solid saturation. An extensive review of this research is available elsewhere[3,4,9], and so a basic review is presented here.

Salars de Atacama and Uyuni brines are characterized as having high concentrations of K^+ and SO_4^{-2}, which can impact significantly, overall lithium solubility and the solid phases that can form. Figure 2 shows the solubility of $Li_2SO_4 \cdot H_2O$, K_2SO_4, and $LiKSO_4$ salts as function of Li_2SO_4 and K_2SO_4 molal concentration. The experimental data is represented by the symbols, and the model predictions are represented by the solid lines. The model is in agreement with experimental data at all temperatures of study. $LiKSO_4$, a mixed-metal salt, is the most stable phase over a broad range of lithium and potassium concentrations. This in turn reduces the overall Li-concentration on the final bittern.

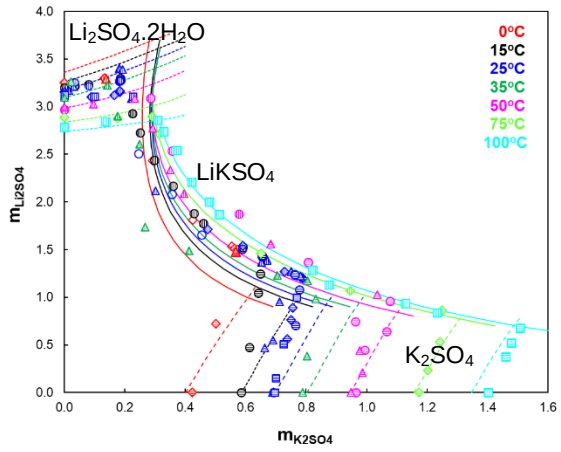

Figure 2. Measured (symbols) vs. predicted (solid lines) solubilities of $Li_2SO_4.H_2O$, K_2SO_4, and $LiKSO_4$ as a function of Li_2SO_4 and K_2SO_4 molal concentrations. Temperature ranges between 0 and 100°C.

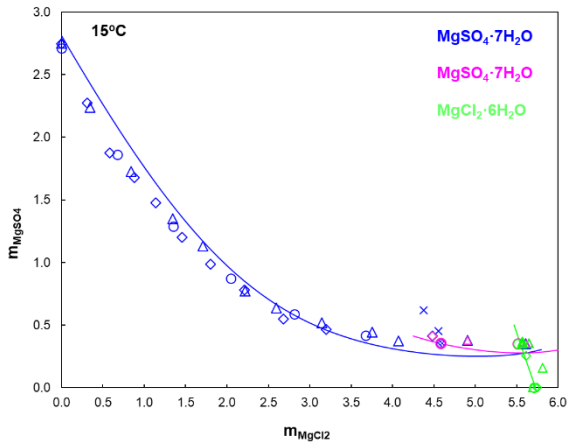

Figure 3. Measured (symbols) vs. predicted (solid lines) solubilities of $MgSO_4·7H_2O$, $MgSO_4·6H_2O$ and $MgCl_2·6H_2O$ salts as a function of $MgSO_4$ and $MgCl_2$ molal concentration at 15°C.

As the evaporation proceeds (later evaporation stages), Salar de Atacama and Salar the Uyuni become high in $MgCl_2$-LiCl and $MgCl_2$-$MgSO_4$. Figure 3, contains the measured and predicted solubility of $MgSO_4·7H_2O$, $MgSO_4·6H_2O$ and $MgCl_2·6H_2O$ salts as a function of $MgSO_4$ and $MgCl_2$ molal concentration at 15 °C. As the $MgCl_2$ salt concentration increases, i.e. as the Cl^{-1}:$SO4^{-2}$ ratio increases, the Mg-sulfate salt transitions from a seven-hydrate to a six-hydrate, and eventually to a six-hydrate Mg-chloride.

Effects of evaporation in a more complex system containing K_2SO_4-$MgSO_4$-KCl-$MgCl_2$-H_2O are presented in Figure 4. As the ratio of SO_4^{-2}:Cl^- and Mg^{2+}:K^+ varies one of seven salt phases may form: KCl (sylvite), KCl.$MgCl_2·6H_2O$ (Carnallite), $K_2Mg(SO_4)_2·6H_2O$ (shoenite), and $KMg(SO_4)Cl·3H_2O$ (kainite). This plot shows the salts that form for a given composition.

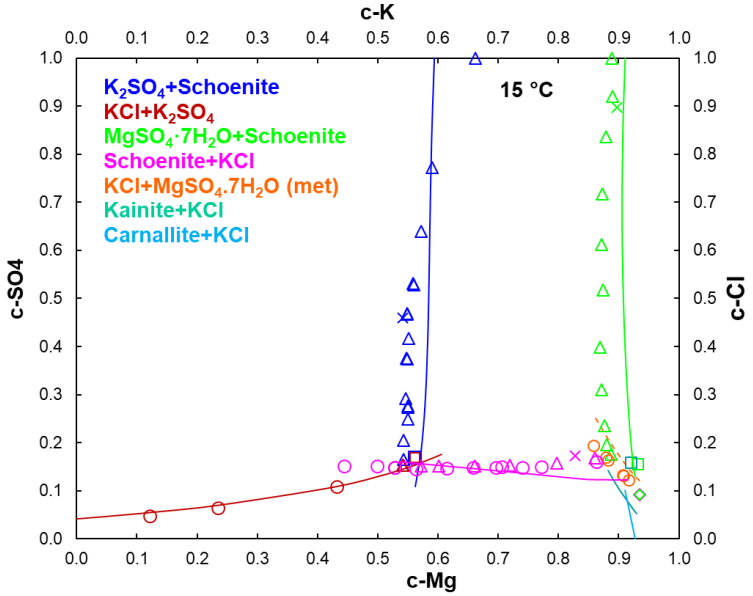

Figure 4. Measured (symbols) and predicted (solid lines) solubilities of the K_2SO_4-$MgSO_4$-KCl-$MgCl_2$-H_2O system as a function of total SO_4^{-2} and Mg^{+2} concentration at 15 °C.

SIMULATING THE SALAR BRINE EVAPORATION PROCESS

Salar brine chemistry appears straightforward because of the simple elements that comprise it: Li^+, Na^+, K^+, Mg^{+2}, and Ca^{+2} metals do not form complex aquo-groups or coordination complexes like transition metals. Additionally, the SO_4^{-2}, $B(OH)_4^-$ and Cl^- anions interact electrostatically with the metals. What make this chemistry complex is the number of possible salts that can form from the combination of these eight ions. Anhydrous salts like NaCl, KCl and $CaSO_4$ are relatively simple to

predict; they are salts of strong acids. However, the 100+ hydrates, double salts, and triple salts that potentially precipitate from these same components creates the complexity, especially as the ion concentrations change and salinities increase. Even within the relatively narrow range of temperature (5-20 °C), pH (4-7), and compositional (saturated NaCl) brines of Andean salars are computed to have about twenty-five salt phases that are at or near saturation (S>0.5).

THE IMPORTANCE OF A SIMULATION TOOL

Solutions of this nature are challenging for computational models because of their complex chemical behavior and strong nonideality. For example, heavy brines like bitterns require mathematical models that incorporate the high ion charge density in the solution, include the concentration and charge effect on molecular H_2O availability, and its dielectric (electrostatic insulation ability). Reduced molecular H_2O availability increases the potential for ion pairs like $MgSO_4^0$ to form, which in turn changes the overall availability of free Mg^{+2} or SO_4^{-2} to precipitate. Reduced molecular H_2O availability also changes the relative solubility of hydrated salts. The net effect is that an anhydrous ($CaSO_4$) or partially hydrated ($CaSO_4.0.5H_2O$) salt may be more likely to form than the hydrated salt ($CaSO_4.2H_2O$), simply because there is no free H_2O to precipitate with the solid. It is for this reason that a comprehensive thermodynamic model and database is needed to predict accurately, the phase equilibria, speciation and other properties during the different steps of lithium extraction.

In addition to SLE and VLE, borate adsorption onto $Mg(OH)_2$ may also be important, should boron be important to the economics of the operation. Adsorption is beyond the scope and will be introduced in a future article. Nevertheless, it is a chemical mechanism that needs to be quantified in order to optimize boric acid yield.

SIMULATION APPROACH AND SALAR BRINES COMPOSITION

Evaporation Simulation of Different Salar Brines

The brines used in the study are presented in Table 1. They represent a distribution of compositions and ion ratios from around the world, and when evaporated, produce a different progression of salt phases. The most important are the Salar de Atacama and Hombre Muerto, where currently there is significant lithium production. Salar de Uyuni is included because of its massive lithium reserves, and some marginal salts from North America are also included.

Table 1. Published and averaged compositions of several Li-bearing brines around the world.*

	Salar de Atacama[1]	***Salar de Hombre Muerto***[1]	***Salar de Uyuni#1***[10]	***Salar de Uyuni#2***[10]	***Salar de Pozuelos***[11]	***Clayton valley***[10]	***Salton Sea***[10]	***Great Salt Lake, US***
Salar #	**1**	**2**	**3**	**4**	**5**	**6**	**7**	**8**
	g/kg	g/kg	g/kg	g/kg	g/kg	g/kg	g/kg	g/kg
Li^+	1.6	0.8	0.65	0.61	0.49	0.16	0.25	0.18
Na^+	90	94.5	82.1	76.0	106.5	46.9	60	62.0
K^+	**24**	5.5	**12.3**	**13.5**	4.8	4.0	**18.5**	4.9
Mg^{+2}	10	1.2	13.1	13.9	2.4	0.19	3.1	7.4
Ca^{+2}	0.5	0.7	2.6	0.27	2.2	4.5	31	0.32
Cl^-	190	158	171.2	160.2	201.5	72.6	171	113.
SO_4^{-2}	16.0	10.5	16.6	18.1	2.6	3.4	4.7	14.7
$B(OH)_3$	**2.3**	**2.5**	**3.5**	**3.1**	0.44	0.29	**2.2**	0.4
HCO_3^{-1}	0.05		0.22	0.16				
Na/Cl Ratio	0.73	0.92	0.8	0.78	0.91	1.00	0.54	0.85

The evaporation simulation is as follows: 1000 m^3 of brine is reduced to 50 m^3 or until a Li-containing salt forms. In this work, the volume reduction is simulated in a 45-step evaporation process, i.e. 45 separate ponds. Dry air (0% H_2O and 400 ppm CO_2) is added at each step to evaporate the brine. Solid phases are removed from the liquid and the remaining brine is transferred to the next step where it interacts with additional air, as is depicted in Figure 5. This scenario is similar to current pond evaporation operations except that many more evaporation ponds are used. The salar brines are

simulated at 10 °C and 0.7 atm. The Clayton Valley, Salton Sea, and Great Salt Lake brines are simulated at 23 C° and 1 atm.

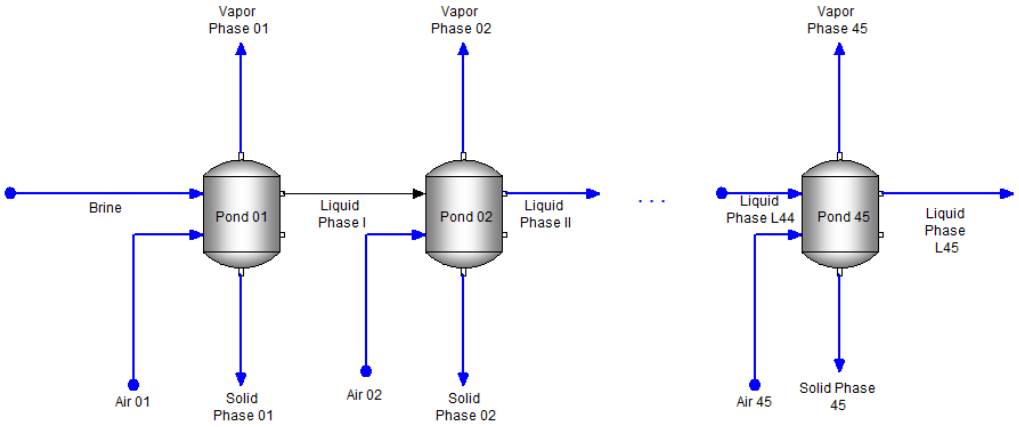

Figure 5. Fractional Crystallization reactor (FCR) scenario, in which the precipitated solids are removed from brine after each evaporation step.

Evaporation Simulation with Chemical Additives

A second set of simulation studies were performed using the above evaporation scenarios plus chemical additives. Additives such as: CaO, Na_2SO_4, and HCl were used to concentrate or reduce targeted elements in solution. The mass and evaporation point where the chemicals are added varied with the optimization scenario.

Solid Phases Considered in the Simulation

Approximately one-hundred forty solids phases were included in all calculations. Of these, twenty-seven salts, including four Li-salts, are computed to form in the eight brines shown in Table 1. These solid phases are displayed Table 2, along with their mineral names (where available), and the number of brines from Table 1 in which these salts are computed to form.

Table 2. Salt that computed to be saturated or nearly saturated during this simulation work.

Formula	Mineral Name	# Brines[a]	Formula	Mineral Name	# Brines[a]
$B(OH)_3$	Boric acid	4	$KMgCl_3.6H_2O$	Carnallte	7
$CaB_6O_{10}.4H_2O$	Nobleite	3	$KClMgSO_4.3H_2O$	Kainite	4
$CaCl_2.2MgCl_2.12H_2O$	Tachyhydrite	2	$Li_2SO_4.H_2O$		4
$CaCl_2.4H_2O$		2	$LiCl.2H_2O$		1
$CaCl_2.6H_2O$	Antarcticite	2	$LiCl.CaCl_2.5H_2O$		2
$CaSO_4$	Anhydrite	8	$LiKSO_4$		1
$CaSO_4.2H_2O$	Gypsum	1	$MgBO_{10}.7.5H_2O$		3
$K_2SO_4.5CaSO_4.H_2O$	Gorgeyite	4	$MgCl_2.6H_2O$	Bischofite	5
$K_2SO_4CaSO_4.H_2O$	Syngenite	4	$MgSO_4.1H_2O$	Kieserite	4
$K_2SO_4.KNaSO_4$	Aphthitalite	1	$MgSO_4.7H_2O$	Epsomite	3
$K_2SO_4.MgSO_4.2CaSO_4.2H_2O$	Polyhalte	4	$Na_2SO_4.CaSO_4$	Glauberite	1
$K_2SO_4.MgSO_4.4H_2O$	Leonite	1	$Na_2SO_4.MgSO_4.4H_2O$		1
$K_2SO_4.MgSO_4.6H_2O$	Schoenite	2	NaCl	Halite	8
KCl	Sylvite	7			

[a] *# Brines: Number of brines from Table 1 where the solids form*

RESULTS

Simulation Results of Evaporation - Salar de Uyuni Sample #1

Figure 6, displays the solids computed to form when 1000 m^3 Salar de Uyuni #1 brine is evaporated to a final liquid volume of 50 m^3. Fourteen salts including $Li_2SO_4.H_2O$ precipitate.

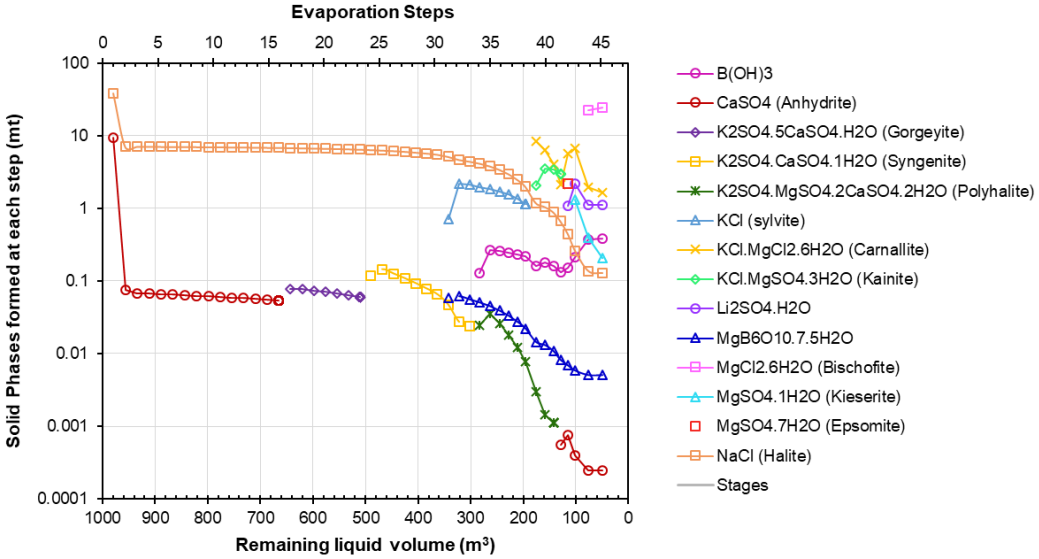

Figure 6. Simulation of the salt phases formed at each evaporation step, when 1000 m^3 Salar de Uyuni #1 is evaporated to 50 m^3 in 45 evaporation steps. The solid phases are separated from the brine at each step and do not participate further in the evaporation process (fractional crystallization scenario).

From Figure 6, it can be seen that halite (NaCl) and anhydrite ($CaSO_4$) precipitate at the first evaporation stage. Halite is computed to precipitate throughout the evaporation process, i.e. in all 45 ponds. At a brine volume of ~120 m^3 (stage 42) the Li-containing salt, $Li_2SO_4.H_2O$, is computed to precipitate. Thus, this simulation predicts that maximum evaporation is about 88%.

The results shown in Figure 6, are also presented in tabular form in Table 3. The total mass (mt) of each salt that precipitated in each step, as the evaporation proceeded. Halite (NaCl) has the highest mass amount, with a total of 262.1 mt, followed by Bischofite ($MgCl_2.6H_2O$), Carnallite ($KCl.MgCl_2.6H_2O$), Sylvite (KCl), Anhydrite ($CaSO_4$) and Kainite ($KCl.MgSO_4.3H_2O$). The total mass of $Li_2SO_4.H_2O$ predicted to form is ~5.5 mt. The total mass of the remaining seven non-Li salts that are predicted to form composed only ~2.3% of the total mass. A total of 397 mt of salt is computed to form.

The purity of each salt, is summarized in Table 3. Halite is 98.5+% pure from initial evaporation (Pond 1) to Pond 28 (360 m^3 liquid). After this point, sylvite (pond 29) and carnallite (pond 38) precipitates reducing the halite purity. By pond 42 (120 m^3 liquid), $Li_2SO_4.H_2O$ is computed to precipitate with epsomite, carnallite, and halite. Its purity is between 4 and 21% depending on the pond.

Table 3. Total mass of each salt forming from 1000 m^3 Salar de Uyuni#1 brine when evaporated to 50 m^3. The salts are separated from the brine after each evaporation step. *when that salt is at least 10% of the combined salt in the pond. **highest purity computed for that salt in any pond

Formula	Mass (mt)	Ponds where salt is found	Average purity*	Maximum purity**
NaCl (Halite)	262.1	1-45	85	99
$MgCl_2.6H_2O$ (Bischofite)	46.2	44-45	86	87
$KCl.MgCl_2.6H_2O$ (Carnallite)	37.0	38-45	56	71
KCl (Sylvite)	14.5	29-37	30	34
$CaSO_4$ (Anhydrite)	19.0	1-14, 41-45	20	20
$KCl.MgSO_4.3H_2O$ (Kainite)	11.8	38-41	34	50
$Li_2SO_4.H_2O$	***5.5***	***42-45***	***16***	***21***
$B(OH)_3$	3.1	32-45		6
$MgSO_4.1H_2O$	1.9	43-45	12	12
$MgSO_4.7H_2O$	2.2	42	23	23
$K_2SO_4CaSO_4.H_2O$	0.8	22-31		3
$K_2SO_4.5CaSO_4.H_2O$	0.5	15-21		2
$MgBO_{10}.7.5H_2O$	0.5	29-45		1
$K_2SO_4.MgSO_4.2CaSO_4.2H_2O$	0.1	32-40		1
Total	**397**			

Figure 7 shows the fraction of each element remaining in the S. de Uyuni #1 brine as the evaporation proceeds. At pond 42 (120 m^3 brine), where lithium precipitates, nearly 100% of Ca^{+2} and Na^+, 80% of K^+ and Cl^-, and 50% of the B^{+3} are removed. The remaining brine is a Mg^{+2} and SO_4^{-2} bittern containing ~5100 ppm lithium.

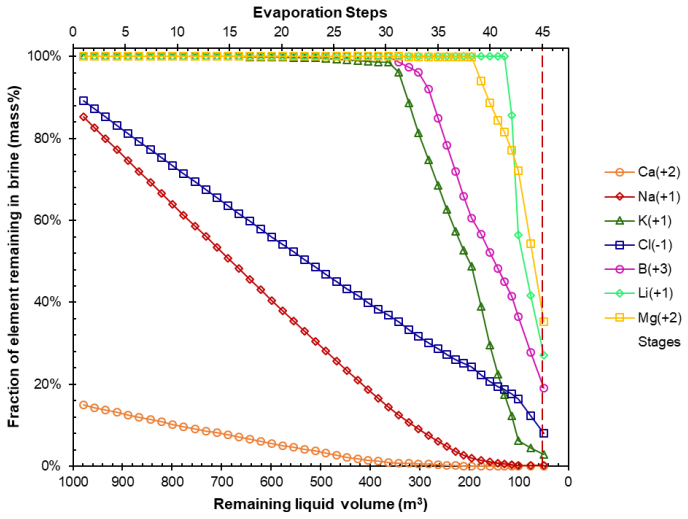

Figure 7. The fraction of element remaining in the Salar de Uyuni #1 brine as solid phases precipitate and are removed (Fractional crystallization scenario)

Removing NaCl Salts in the First Part of the Evaporation

Halite, NaCl, precipitates first in every brine except Clayton Valley and Great Salt Lake, where calcium sulfates form first. The fraction of evaporation where NaCl (>98% purity) precipitates is presented in Table 4.

The first three rows are: total mass of NaCl formed, NaCl purity, and the volume of brine remaining. Salar de Hombre Muerto, for example, can be evaporated from 1000 m^3 to 109 m^3 in a single pond, and the halite harvested from that pond will have a purity of 98.6%. The composition of the remaining

brine is shown in the lower part of the table. The final two rows are the computed brine volume where Li-salt start to precipitate, and the concentration of lithium in the brine.

Table 4- Updated salar composition in the middle of evaporation where halite is removed and solids are about to precipitate.

	S. de Atacama	S. de Hombre Muerto	S. de Uyuni#1	S. de Uyuni#2	S. de Pozuelos	Clayton Valley[1]	Salton Sea	Great Salt Lake, US
NaCl Salt formed (mt)	209	282	224	204	293	113	142	152
NaCl Purity (%)	98.2	98.6	95.1	99.1	98.6	99.5	94.5	99.1
Remaining brine (m^3)	551	109	363	352	205	99	504	204
Remaining Brine composition, g/kg								
Li^+	2.9	6.3	1.8	1.6	2.4	1.4	0.5	0.8
Na^+	51.8	62.5	32.2	30.3	60.2	55.6	28.6	46.8
K^+	42.5	44.6	32.5	35.7	23	35.1	35.3	21.5
Mg^{+2}	18.1	9.9	35	37.4	11.5	1.7	5.9	32.6
Ca^{+2}	0.1	0	0.1	0	6.0	27.2	55.5	0
Cl^-	167.1	145	169.8	162.3	169.2	178	194	145.9
SO_4^{-2}	25.9	72.1	27.6	46.3	1.2	0.3	0.1	61.1
$B(OH)_3$	4.1	16.4	29.4	8	11.7	2.5	4.3	1.8
Na:Cl mole ratio in remaining brine	0.48	0.66	0.29	0.28	0.55	0.48	0.23	0.49
Volume where Li^+ precipitate	104	50	115	100	8.4	3.1	6.9	40
Concentration of Li^+ at ppt point	13400	13100	5110	5400	48400	37300	28400	3800

Potash and Boric acid recovery following NaCl removal

Figure 8 is a plot showing the K^+ purity in precipitating salts starting from the remaining brine volume (Table 4) to the final evaporation point (either 50 m^3, or when Li-salts form, whichever is smaller). The brine creating a salt mixture with the highest K-content is Salton Sea, where between ~500 m^3 and 220 m^3, the K-content ranges from 20 to 30 mass%. The K-bearing salt phases that form are provided in Table 2.

Salar de Atacama produces appreciable K-salts at the highest remaining volume, 551 m^3 (Table 4). Potassium salts continue to precipitate in appreciable amounts until about 175 m^3, and the salts are about 15% potassium.

A similar plot for boron is provided in Figure 9. Boron is roughly one-fourth the mass of potassium and so the percentages are lower. If the goal is to keep boron in solution so that it could be extracted efficiently, then chemical addition is required to remove Mg in another form, e.g. $MgSO_4$, or $MgCO_3$.

[1] Clayton Valley – NaCl does not start precipitating until 54% of the brine has evaporated. Up to this point $CaSO_4.2H_2O$ and $CaSO_4$ precipitates.

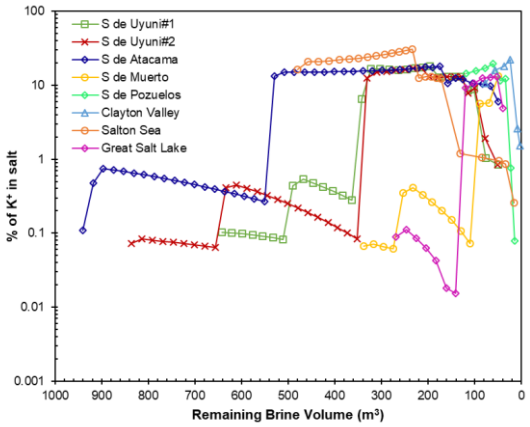

Figure 8 - Percentage of metal in the salt that is K^+ (Cl, SO_4, and salt-H_2O masses are excluded). The values are calculated at each evaporation step.

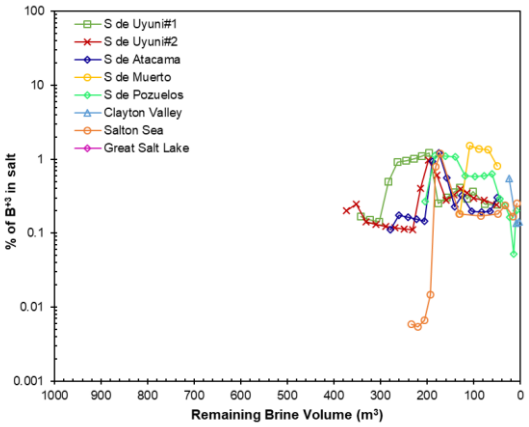

Figure 9 - Percentage of B as a function of total metals in the precipitating salts. The salts form downstream of the NaCl removal. The curves are the percentage of B in the salt within each of the simulated ponds. One curve is for each of the nine brines in this study.

CHEMICAL ADDITIVES TO MODIFY SALT FORMATION IN SALAR DE ATACAMA

Maximizing potassium and boron yield and purity requires modifications to the brine composition. Two potential approaches include:

1. Adding elements so that their molar ratio with the precipitating ion approaches 1:1. For instance, all brines have Na:Cl ratios that are below 1:1. Therefore by adding Na^+ to raise the molar ratio and precipitate more NaCl will reduce the formation of other metal chlorides.

2. Adding elements so that their molar ratio with the precipitating ion deviates from unity. For instance, raising the calcium concentration so that the Ca:SO_4 ratio >>1. This eliminates sulfate salts like $LiKSO_4$ or $Li_2SO_4.H_2O$ from precipitating.

Table 5 below contains simulation runs on the Salar de Atacama brine using the following additives.

1. 40 m^3 35% HCl at evaporation step #0

2. 10 mt Na_2SO_4 at evaporation step #0

3. 20 mt $NaNO_3$ at evaporation step # 0

Table 5 – Chemicals added to the Atacama brine for the purpose of producing K-salts, boric acid and NaCl with higher purity.

Variable	Units	Base	HCl	Na_2SO_4	$NaNO_3$
NaCl mass before K-salts start to precipitate	Kg	206	194	221	225
NaCl purity before K-salts start to precipitate	%	98.2	99.7	97.8	98.8
Recoverable Potash (after main NaCl)	mt as K	29	30	29	30
K purity in potash (after main NaCl)	wt% K	12.9	12.5	13.1	14.3
Recoverable boric acid	mt	1.68	2.81	2.9	2.9
Value of salable boric acid after purified	$	1210	2,023	2,080	2,080
Chemical cost	$	0	5,000	1,000	$8,000

Each approach has drawbacks in chemical cost, and undesirable salts that form as a result of changing these ratios. For instance, adding Ca^{+2} causes calcium borates to precipitate, reducing the boric acid yield. Adding Na^{+} in the form of Na_2SO_4, $NaNO_3$, $NaHCO_3$, or NaOH increases the Na:Cl ratio. This has the benefit of increasing NaCl yield and reducing the formation of other chlorides (e.g. carnallite). Depending on the additive, it can also causes double salts and triple salts form with of K-Mg-Ca to form and can reduce potash yield. For example,

- Adding $NaNO_3$ delays K precipitation and produces a salable KNO_3 product. This is costly, and only a limited amount of $NaNO_3$ can be added before KNO_3 precipitates as a minor constituent in the NaCl salt bed.
- Adding $NaHCO_3$ and NaOH causes Ca- and Mg-borates to precipitate as minor salts in NaCl beds, reducing boric acid yields. Also, NaOH is expensive.
- Adding HCl increases NaCl formation early in the evaporation process. It eventually leads to KCl and $KCl.MgCl.3H_2O$ formation.

The 2018 price range for salt products or chemical additives considered are shown in Table 6 and were used to calculate the total cost of producing Boric Acid in Table 5.

Table 6 - Prices for various commodity chemicals.

Salt	Price per ton ($US)	Additive	Price per ton ($US)
$B(OH)_3$	$720[14]	NaOH	$400-500[15]
NaCl	$20-70[16]	HCl (35%)	$100[17]
KNO_3	$700	$NaNO_3$	$400
Na_2SO_4	$100[13]		

SUMMARY

The development of the thermodynamics of heavy brine chemistry has advanced to the point where modeling salar evaporation can be done with reasonable effectiveness. Experimental data and phases available for the subsystems of Li-Na-K-Mg-Ca-B-SO_4-CO_3-Cl was presented and were used to calibrate the MSE thermodynamic framework to represent these systems. Simulation results for the evaporation process of eight Li-containing natural brines, including the salt phases predicted to form as evaporation progresses, were presented. Different what-if scenarios that predict the effects of chemical additives on salt phase formation, and how it can be manipulated to isolate K- and B-containing salts were investigated. It is important to highlight that these simulation predictions do not include the effects of mass-transfer limitations nor rate-limited precipitation on overall results.

REFERENCES

1. Valdez, S., Flores, H., Orce, A. & Kwokleung, H. Influence of The Evaporation Rate Over Lithium Recovery From Brines. *World J. Res. Rev.* **3,** 66–70 (2016).
2. Wang, P., Anderko, A. & Young, R. D. A speciation-based model for mixed-solvent electrolyte systems. *Fluid Phase Equilib.* **203,** 141–176 (2002).
3. Wang, P., Kosinski, J. J., Lencka, M. M., Anderko, A. & Springer, R. D. Thermodynamic modeling of boric acid and selected metal borate systems*. *Pure Appl. Chem* **85,** 2117–2144 (2013).
4. Wang, P., Anderko, A., Springer, R. D., Kosinski, J. J. & Lencka, M. M. Modeling chemical and phase equilibria in geochemical systems using a speciation-based model. *J. Geochemical Explor.* **106,** 219–225 (2010).
5. Wang, P., Anderko, A., Springer, R. D. & Young, R. D. Modeling phase equilibria and speciation in mixed-solvent electrolyte systems: II. Liquid-liquid equilibria and properties of associating electrolyte solutions. *J. Mol. Liq.* **125,** 37–44 (2006).

6. Helgeson, H. C., Kirkham, D. H. & Flowers, G. C. Theoretical prediction of the thermodynamic behavior of aqueous electrolytes by high pressures and temperatures; IV, Calculation of activity coefficients, osmotic coefficients, and apparent molal and standard and relative partial molal properties. *Am. J. Sci.* **281,** 1249–1516 (1981).

7. Tanger, J. C. & Helgeson, H. C. Calculation of the thermodynamic and transport properties of aqueous species at high pressures and temperatures; revised equations of state for the standard partial molal properties of ions and electrolytes. *American Journal of Science* **288,** 19–98 (1988).

8. Soave, G. Equilibrium constants from a modified Redlich-Kwong equation of state. *Chem. Eng. Sci.* **27,** 1197–1203 (1972).

9. Anderko, A., Wang, P., Springer, R. D., Lencka, M. M. & Kosinski, J. J. Prediction of Mineral Scaling in Oil and Gas Production using a Comprehensive Thermodynamic Model. *NACE Int.* Paper No.10129 (2010).

10. An, J. W. *et al.* Recovery of lithium from Uyuni salar brine. *Hydrometallurgy* **117–118,** 64–70 (2012).

11. Hains, D. H. Technical Report on the Salar De Pozuelos Project , Salta Province , Argentina Prepared for Lsc Lithium Corporation. *Hains Eng. Co. Ltd.* (2017).

12. Potassium Chloride Monthly Price - US Dollars per Metric Ton. *Index Mundi* (2019). Available at: https://www.indexmundi.com/commodities/?commodity=potassium-chloride.

13. Chemical profile: Sodium sulfate. *ICIS* (2019). Available at: https://www.icis.com/explore/resources/news/2007/09/10/9060326/chemical-profile-sodium-sulfate/.

14. Medium-term forecast for boric acid prices worldwide from 2012 to 2023 (in U.S. dollars per metric ton). *Statista* (2019). Available at: https://www.statista.com/statistics/449813/global-prediction-of-medium-term-boric-acid-prices/.

15. US caustic soda spot export prices return to pre-Hurricane Harvey level. *ICIS* (2019). Available at: https://www.icis.com/explore/resources/news/2018/10/20/10267616/us-caustic-soda-spot-export-prices-return-to-pre-hurricane-harvey-level/.

16. Sodium Chloride Price per Ton. *Alibaba.com* (2019). Available at: https://www.alibaba.com/showroom/sodium-chloride-price-per-ton.html.

17. OUTLOOK ’18: US HCl poised for demand surge in new year. *ICIS* (2019). Available at: https://www.icis.com/explore/resources/news/2018/01/03/10173417/outlook-18-us-hcl-poised-for-demand-surge-in-new-year/?redirect=english.